THE JOURNAL OF BIOLOGICAL CHEMISTRY VOL. 284, NO. 45, pp. 31214–31222, November 6, 2009

Involvement of Ionizable Groups in Catalysis of Human Liver Glycolate Oxidase*[S]

Received for publication, July 2, 2009, and in revised form, September 4, 2009 Published, JBC Papers in Press, September 16, 2009, DOI 10.1074/jbc.M109.040063

Andrea Pennati[‡] **and Giovanni Gadda**[‡§¶1]

From the Departments of [‡]*Chemistry and* [§]*Biology and* [¶]*Center for Biotechnology and Drug Design, Georgia State University, Atlanta, Georgia 30302-4098*

Glycolate oxidase is a flavin-dependent, peroxisomal enzyme that oxidizes α-hydroxy acids to the corresponding α-keto acids, with reduction of oxygen to H_2O_2. In plants, the enzyme participates in photorespiration. In humans, it is a potential drug target for treatment of primary hyperoxaluria, a genetic disorder where overproduction of oxalate results in the formation of kidney stones. In this study, steady-state and pre-steady-state kinetic approaches have been used to determine how pH affects the kinetic steps of the catalytic mechanism of human glycolate oxidase. The enzyme showed a Ping-Pong Bi-Bi kinetic mechanism between pH 6.0 and 10.0. Both the overall turnover of the enzyme (k_{cat}) and the rate constant for anaerobic substrate reduction of the flavin were pH-independent at pH values above 7.0 and decreased slightly at lower pH, suggesting the involvement of an unprotonated group acting as a base in the chemical step of glycolate oxidation. The second-order rate constant for capture of glycolate ($k_{cat}/K_{glycolate}$) and the $K_{d(app)}$ for the formation of the enzyme-substrate complex suggested the presence of a protonated group with apparent pK_a of 8.5 participating in substrate binding. The k_{cat}/K_{oxygen} values were an order of magnitude faster when a group with pK_a of 6.8 was unprotonated. These results are discussed in the context of the available three-dimensional structure of GOX.

Glycolate oxidase (EC 1.1.3.15; glycolate:oxygen oxidoreductase; GOX)[2] catalyzes the FMN-mediated oxidation of glycolate to glyoxylate with reduction of oxygen to hydrogen peroxide (Scheme 1) (1). The enzyme has been identified in plants and mammals and contains tightly but not covalently linked FMN. GOX has been grouped in the superfamily of the α-hydroxy acid oxidases, which includes among others long-chain hydroxy acid oxidase, lactate oxidase, mandelate dehydrogenase, and the flavin-binding domain of yeast flavocytochrome b_2 (2–6). In plants, GOX is localized in the glyoxysome of photosynthetic tissues, where it participates in photorespiration (7, 8). In humans and other vertebrates, such as pigs, the enzyme is found in the peroxisomes of liver and kidney and is involved in the production of oxalate (9–11). The latter finding recently prompted considerable interest in the study of the mechanistic and structural properties of human GOX for the potential development of therapeutic agents targeting the treatment of primary hyperoxaluria (12), a genetic disorder in which overproduction of oxalate results in large deposits of calcium oxalate.

To date, the GOX that is best characterized in its structural, kinetic, and biochemical properties is the one from spinach leaves (13–19). Recently, the structure of the enzyme from human liver has been solved in complex with a number of ligands to resolutions of ≤1.95 Å (20). In the active site of the human enzyme (Fig. 1), and based on mutational studies on the spinach enzyme, mandelate dehydrogenase, or flavocytochrome b_2, Tyr^{26}, Arg^{167}, and Arg^{263} have been proposed to participate in the binding of the carboxylate group of glyoxylate (19–22). Based on its spatial location in the active site, His^{260} has been proposed to initiate catalysis by acting as the proton acceptor for the deprotonation of the hydroxyl group or the α-carbon of the substrate (19, 20). However, mechanistic studies on human GOX have yet to address such proposals. Apparent steady-state kinetic parameters with glycolate as substrate for human liver GOX have been reported by other research groups for pH 7.0 and 7.5 at atmospheric concentration of oxygen (1, 23). The enzyme has been reported to be inhibited by chloride ions, oxalate and mandelate, with IC_{50} values of 280, 1.8, and 3.7 mM, respectively, at pH 7.0 and 25 °C, and to form a reversible covalent FMN-adduct with sulfite, with a K_d value of ~60 μM at pH 7.0 and 25 °C (23).

In this study, we have determined the steady-state and pre-steady-state kinetic parameters with glycolate as substrate for human liver GOX in the pH range from 5.0 to 10.0. The enzyme showed a Ping-Pong Bi-Bi steady-state kinetic mechanism throughout the pH range considered, with the requirement of a protonated group for binding of the substrate in the active site. The kinetic step in which substrate oxidation results in the reduction of the flavin was independent of pH above pH 7.0, with a slight decrease at lower pH values, consistent with the presence of an unprotonated group participating in the chemical step of glycolate oxidation. The k_{cat}/K_{oxygen} values increased between two limiting values with increasing pH, identifying an unprotonated group with pK_a of 6.8 that is important for flavin oxidation. Finally, the overall turnover of the enzyme is limited by the chemical step of flavin reduction at high pH and by another kinetic step at low pH.

* This work was supported in part by National Science Foundation Career Award MCB-0545712 (to G. G.).

[S] The on-line version of this article (available at http://www.jbc.org) contains supplemental Fig. S1.

[1] To whom correspondence should be addressed: Chemistry Dept., Georgia State University, P.O. Box 4098, Atlanta, GA 30302-4098. Tel.: 404-413-5537; Fax: 404-413-5551; E-mail: ggadda@gsu.edu.

[2] The abbreviation used is: GOX, glycolate oxidase.

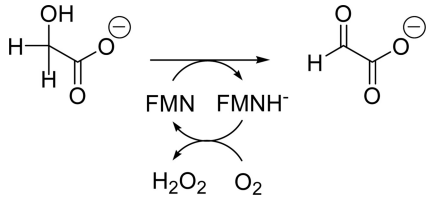

SCHEME 1. **Oxidation of glycolate catalyzed by human liver GOX.**

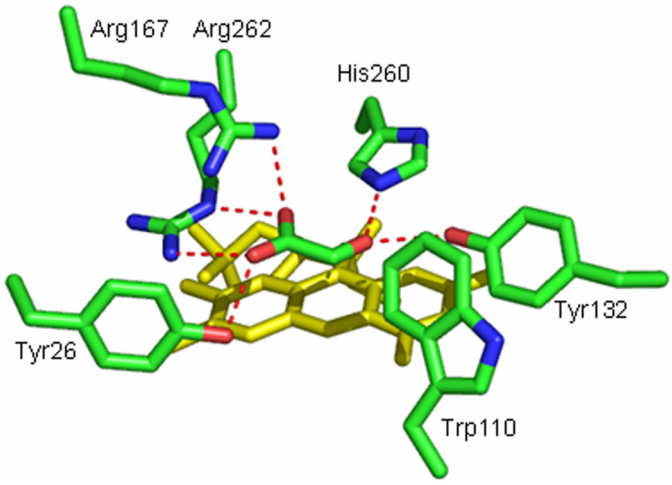

FIGURE 1. **Active site of human liver GOX (Protein Data Bank 2RDU).** The *dotted lines* represent proposed hydrogen bonding and electrostatic interactions of selected amino acid residues in the active site of the enzyme with glyoxylate.

EXPERIMENTAL PROCEDURES

Materials—The plasmid pTrcHisB-*HAOX1* harboring the gene encoding for human liver GOX was a gift from Prof. Peracchi (University of Parma, Italy). *Escherichia coli* strain Rosetta(DE3)pLysS was from Novagen (Madison, WI). DNase was from Roche Applied Science. Bovine serum albumin, chloramphenicol, DMSO, isopropyl β-D-thiogalactopyranoside, phenylmethanesulfonyl fluoride, lysozyme, glycolate, glucose, glucose oxidase from *Aspergillum niger*, Luria-Bertani agar, and broth were from Sigma. EDTA was from Fisher. Ampicillin was from ICN Pharmaceutical Inc. Nickel-Sepharose high performance and PD-10 columns were from GE Healthcare. All other reagents were of the highest purity commercially available.

Expression of Human GOX in E. coli—GOX was expressed following a modification of the procedure previously published (23, 24). *E. coli* Rosetta(DE3)pLysS cells were transformed with pTrcHisB-*HAOX1* and permanent stocks of these transformants were stored at −80 °C. Colonies of transformants, which were selected on Luria-Bertani plates supplemented with 50 μg/ml ampicillin and 34 μg/ml chloramphenicol were transferred in 50 ml of Luria-Bertani broth medium containing the same antibiotics. The culture was grown at 37 °C under orbital shaking (220 rpm). After 3 h, 10 ml of the starter culture were used to inoculate 5 × 1 liter of the same liquid culture medium at 37 °C, 220 rpm. When the culture reached an optical density at 600 nm of 0.6, typically after 5 h, isopropyl β-D-thiogalactopyranoside was added to a final concentration of 0.5 mM. Expression of GOX was induced at 37 °C for 16 h. Cells were harvested by centrifugation at 5,000 × *g* for 20 min at 4 °C and stored at −20 °C until used for enzyme purification.

Purification of Recombinant Human GOX—All of the purification steps were carried out at 4 °C. The cell paste, typically 20 g, was suspended in 4 volumes of 50 mM sodium phosphate, pH 7.4, containing 500 mM NaCl, 20 mM imidazole, 10% glycerol, 0.2 mg/ml lysozyme, and 1 mM phenylmethanesulfonyl fluoride. After sonication for a total of 15 min in a Fisher sonifier, the cell-free extract was obtained by centrifugation for 30 min at 20,000 × *g*. The soluble fraction was loaded onto a nickel-Sepharose high performance (GE Healthcare) column (25 ml) connected to an Äkta*prime* Amersham Biosciences system equilibrated in 50 mM sodium phosphate, pH 7.4, containing 500 mM NaCl, 20 mM imidazole, and 10% glycerol. Unbound proteins were removed by washing the column with 100 ml of equilibrating buffer, followed by a linear gradient from 20 to 500 mM imidazole developed over 10 column volumes. The fractions with the highest purity as judged by UV-visible absorbance spectroscopy were pooled together and were concentrated with the addition of 70% ammonium sulfate saturation followed by centrifugation. The pellet was solubilized and dialyzed against 50 mM sodium phosphate, pH 7.0, containing 100 mM NaCl[3] and 10% glycerol. Aliquots of the solution containing the enzyme, after removal of the precipitated protein by centrifugation, were stored at −20 °C.

Site-directed Mutagenesis and Purification of Human Liver H260A and H260Q Enzymes—The enzyme variants where His^{260} is replaced with glutamine or alanine were prepared using the QuikChange site-directed mutagenesis kit (Stratagene), following the manufacturer's instructions. After confirming the mutations by DNA sequencing at the DNA Core Facility at Georgia State University, the mutated enzymes were expressed (at 37 or 20 °C) and purified as described above for the wild-type enzyme.

Enzyme Assays—GOX activity was measured with the method of the initial rates (25) using a computer-interfaced Oxy-32 oxygen-monitoring system (Hansatech Instruments Ltd.) thermostated at 30 °C. Steady-state kinetic parameters for GOX were determined at varying concentrations of glycolate between 0.05 and 20 mM and oxygen between 0.1 and 1 mM. The pH dependences of the steady-state kinetic parameters of GOX were determined by measuring enzymatic activity at varying concentration of both glycolate and oxygen. Sodium phosphate (100 mM final) was used in the pH range from 6.0 to 8.0, and sodium pyrophosphate (100 mM final) was used in the pH range from 8.5 to 10.0. When both glycolate and oxygen were varied, the assay reaction mixture was equilibrated at the desired concentration of oxygen by bubbling the appropriate O_2/N_2 gas mixture for 10 min before the reaction was started by the addition of the enzyme.

The effects of solvent viscosity on the $k_{cat}/K_{glycolate}$ values were measured in air-saturated 100 mM sodium phosphate, pH

[3] Although chloride ions at high concentrations inhibit GOX (IC_{50} value of 280 mM at pH 7.0, 25 °C; see Ref. 24), the final concentration of NaCl that was carried over to the assay reaction mixtures for the measurement of steady-state kinetic parameters was typically ≤0.5 mM, thereby resulting in negligible effects on the determination of the initial rates of reaction. As described under "Experimental Procedures," the enzyme used for anaerobic flavin reduction experiments with a stopped-flow spectrophotometer was freshly prepared prior to use by gel filtration through PD10 columns equilibrated with the proper buffers devoid of NaCl.

7.0, at 30 °C, using glycerol as viscosigen. The values for the relative viscosities at 30 °C were calculated according to the values at 25 °C from Lide (26).

Stopped-flow studies of the reductive half reaction catalyzed by GOX were performed at 30 °C using a Hi-Tech Scientific SF-61 DX2 stopped-flow spectrophotometer under anaerobic conditions. GOX aliquots were gel-filtered through a PD-10 column (GE Healthcare) against 100 mM piperazine at pH 5.0, 100 mM sodium phosphate in the pH range from 6.0 to 8.0 and 100 mM sodium pyrophosphate in the pH range from 9.0 to 10.0. The solution of enzyme was made anaerobic in a tonometer by repeated cycles of evacuation and flushing with oxygen-free argon (pretreated with an oxygen scrubbing cartridge (Agilent, Palo Alto, CA)). Next, the tonometer containing the anaerobic enzyme was mounted onto the stopped-flow instrument, which had been subjected to an overnight incubation with an oxygen scrubbing system containing glucose (5 mM) and glucose oxidase (3,600 units). Glycolate solution were prepared in the same buffer systems used for GOX at concentrations ranging from 0.125 to 40 mM and were made anaerobic by flushing with oxygen-free argon for at least 15 min before mounting the syringe with the substrate onto the stopped-flow instrument. To scavenge possible trace amounts of oxygen in the enzyme and substrate, glucose (2 mM) and glucose oxidase (0.5 μM) were present. Equal volumes of GOX and substrate were mixed anaerobically in the stopped-flow apparatus, yielding a final enzyme concentration of ~20 μM. Triplicate measurements differed typically by less than 2%.

Data Analysis—Kinetic data were fit with KaleidaGraph software (Synergy Software, Reading, PA) and GraFit 5 (Erythacus Software Ltd., Staines, UK). The steady-state kinetic parameters were determined by fitting the initial rates of reactions to Equation 1, which describes a Ping-Pong Bi-Bi kinetic mechanism. K_a and K_b are the Michaelis constants for glycolate (A) and oxygen (B), respectively, and k_{cat} is the turnover number of the enzyme (e) when saturated with both substrates.

$$\frac{v}{e} = \frac{k_{cat}AB}{K_aB + K_bA + AB} \quad \text{(Eq. 1)}$$

Product inhibition studies were performed by varying the concentrations of both glycolate (from 0.02 to 1.0 mM) and glyoxylate (0, 0.5, 1.0, and 2.5 mM) at a fixed atmospheric concentration of oxygen. The data were fit to Equation 2, which describes an uncompetitive inhibition pattern of the product and the organic substrate. A is the concentration of glycolate, P is the concentration of glyoxylate, and K_{ii} is the inhibition constant for binding of glyoxylate to GOX.

$$\frac{v}{e} = \frac{k_{cat}A}{K_a + A\left(1 + \left(\frac{P}{K_{ii}}\right)\right)} \quad \text{(Eq. 2)}$$

The pH profile of the $k_{cat}/K_{glycolate}$ values was determined by fitting the data to Equation 3, which describes a curve with a slope of −1 and a plateau region at low pH. C is the pH-independent value of the kinetic parameter of interest. The pH profile of the k_{cat}/K_{oxygen} value was determined by fitting the data to Equation 4, where Y_L and Y_H are the limiting values at low and high pH, respectively, and K_a is the dissociation constant for the ionization of groups that are relevant to catalysis.

$$\mathrm{Log}Y = \log\left(\frac{C}{1 + \frac{10^{-pK_a}}{10^{-pH}}}\right) \quad \text{(Eq. 3)}$$

$$\mathrm{Log}Y = \log\left(\frac{Y_L + Y_H\left(\frac{10^{-pK_a}}{10^{-pH}}\right)}{1 + \frac{10^{-pK_a}}{10^{-pH}}}\right) \quad \text{(Eq. 4)}$$

Stopped-flow traces at individual wavelengths were fit to Equation 5, which describes a double exponential process, using KinetAsyst 3 software (Hi-Tech Scientific). A is the value of absorbance at the specific wavelength of interest, k_{obs1} and k_{obs2} are the observed first-order rates for the phases of the reaction, B_1 and B_2 are the corresponding amplitudes for the change in absorbance associated with the phase of interest, and C is an offset value to account for a non-zero final absorbance value. Pre-steady-state kinetic parameters were determined by using Equations 6 and 7, where k_{obs} is the observed first-order rate for the reduction of the enzyme-bound flavin at any given concentration of substrate, k_3 is the limiting first-order rate constant for flavin reduction at saturating substrate concentration, k_{rev} is the rate constant for the reverse step in catalysis, and $K_{d(app)}$ is the apparent dissociation constant for the enzyme-substrate complex, which is equal to $(k_2 + k_3)/k_1$ (see "Results"). The pH profile of the $K_{d(app)}$ values for glycolate was determined by fitting the individual $K_{d(app)}$ values to Equation 8, which describes a curve with a slope of +1 and a plateau region at low pH. C is the pH-independent value of $K_{d(app)}$.

$$A = B_1\exp(-k_{obs1}t) + B_2\exp(-k_{obs2}t) + C \quad \text{(Eq. 5)}$$

$$k_{obs} = \frac{k_3[\text{glycolate}]}{K_{d(app)} + [\text{glycolate}]} + k_{rev} \quad \text{(Eq. 6)}$$

$$k_{obs} = \frac{k_3[\text{glycolate}]}{K_{d(app)} + [\text{glycolate}]} \quad \text{(Eq. 7)}$$

$$\mathrm{Log}Y = \log(C(1 + 10^{-pK_a + pH})) \quad \text{(Eq. 8)}$$

The viscosity effects data on the $k_{cat}/K_{glycolate}$ values were fit to Equation 9, where $(k_{cat}/K_{glycolate})_o$ and $(k_{cat}/K_{glycolate})_\eta$ are the values in the absence and presence of viscosigen, S is the degree of viscosity dependence, and η_{rel} is the relative viscosity.

$$\frac{(k_{cat}/K_{glycolate})_o}{(k_{cat}/K_{glycolate})_\eta} = S(\eta_{rel} - 1) + 1 \quad \text{(Eq. 9)}$$

RESULTS

Expression and Purification of Recombinant Human Liver GOX—Heterologous expression of GOX was performed using Rosetta(DE3)pLysS as the host strain, by inducing the cultures at 37 °C overnight with 0.5 mM isopropyl β-D-thiogalactopyranoside. GOX was purified on nickel affinity chromatography after optimizing the conditions in order to maximize the recovery of the enzyme in holoprotein form. Indeed, initial attempts

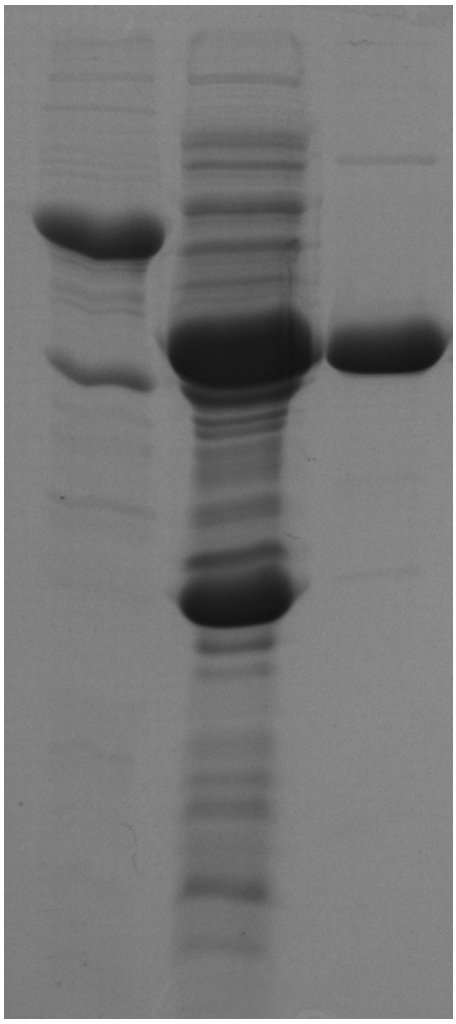

FIGURE 2. **Purification of recombinant human liver GOX heterologously expressed in *E. coli* Rosetta(DE3)PLysS as analyzed by SDS-PAGE.** *Lane 1*, molecular mass marker choline oxidase from *Arthrobacter globiformis* (60 kDa) and 2-nitropropane dioxygenase from *Neurospora crassa* (40 kDa). *Lane 2*, cell-free extract. *Lane 3*, purified GOX.

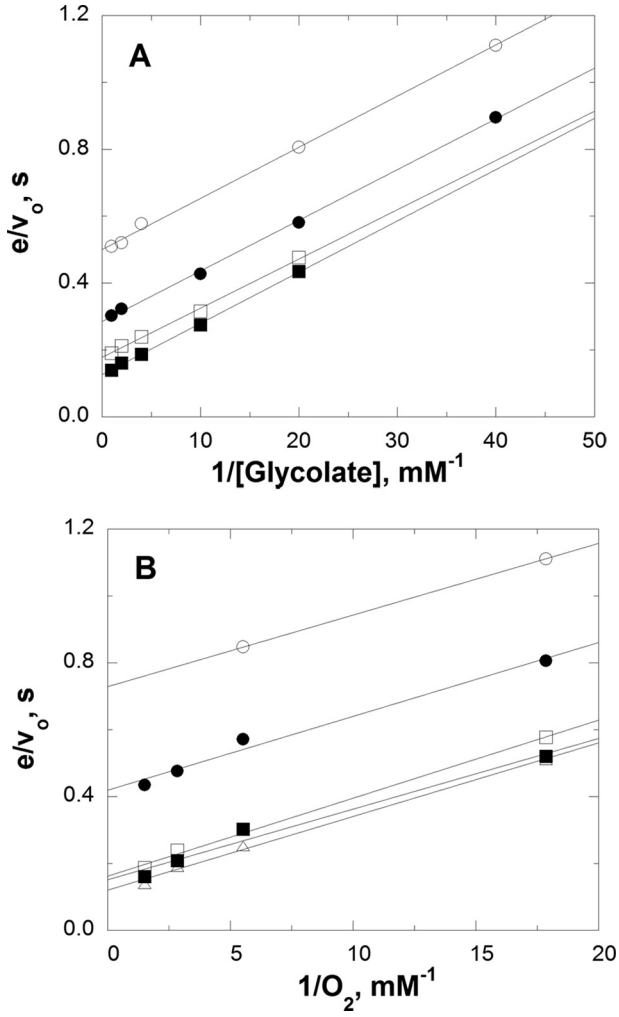

FIGURE 3. **Double reciprocal plots of the oxidation of glycolate catalyzed by human liver GOX at pH 7.0 and 30 °C.** Initial rates of reaction were measured at varying concentrations of both glycolate and oxygen in 100 mM sodium phosphate, pH 7.0, at 30 °C. *A*, *e/v* as a function of the inverse glycolate concentration determined at a fixed concentration of oxygen. ○, 0.054 mM; ●, 0.181 mM; □, 0.352 mM; ■, 0.858 mM oxygen. *B*, *e/v* as a function of the inverse oxygen concentration determined at several fixed concentrations of glycolate. ○, 0.05 mM; ●, 0.1 mM; □, 0.25 mM; ■, 0.5 mM; △, 1 mM glycolate. The *lines* in *A* and *B* are from the global fit of the kinetic data to Equation 1.

yielded significant amounts of free FMN originating from the enzyme during the washing of the column. Glycerol, salts, and neutral pH turned out to substantially stabilize the native conformation of GOX without loss of bound FMN. Consequently, 10% glycerol was included in all the solutions used throughout the purification procedure, whereas the enzyme storage buffer was supplemented with 100 mM NaCl.[3] Following this procedure, ~8 mg of GOX were routinely purified to high levels (Fig. 2) out of 1 g of wet cell paste, with a specific activity of ~4.0 units/mg using 10 mM glycolate and atmospheric oxygen at pH 7.0 and 30 °C.

Kinetic Mechanism and Parameters at pH 7.0—The steady-state kinetic mechanism and the associated kinetic parameters of the enzyme were determined using the method of the initial rates by measuring the rates of oxygen consumption at varying concentrations of both glycolate and oxygen in 100 mM sodium phosphate, pH 7.0, at 30 °C. Initial velocity data yielded parallel lines in double reciprocal plots (Fig. 3), suggesting a Ping-Pong Bi-Bi kinetic mechanism in which the enzyme-bound FMN is alternately reduced by glycolate and reoxidized by oxygen. Fitting of the kinetic data to Equation 1 yielded an overall turnover number (k_{cat}) of 15.7 ± 0.4 s^{-1}, a second-order rate constant for the capture of glycolate ($k_{cat}/K_{glycolate}$) of 68,300 ± 3,500 M^{-1} s^{-1}, and a second-order rate constant for reaction of the reduced flavin with oxygen (k_{cat}/K_{oxygen}) of 24,500 ± 1,300 M^{-1} s^{-1}. In contrast to a recent report, we did not observe enzyme inhibition at concentrations of glycolate as high as 20 mM (23).

As a complementary approach to establish the order of binding of substrates and products to the enzyme, the inhibition pattern of the product of the reaction, glyoxylate, *versus* glycolate was determined in 100 mM sodium phosphate, pH 7.0, using the steady-state kinetics approach at atmospheric oxygen concentration. The inhibitor concentrations were varied between 0.5 and 2.5 mM, which is below the K_m value for glyoxylate of 3.4 mM reported for the same enzyme at pH 7.0 (23). As shown in Fig. 4, a double reciprocal plot of the initial rates of reaction as a function of the substrate concentration at fixed concentrations of product yielded parallel lines. The observed

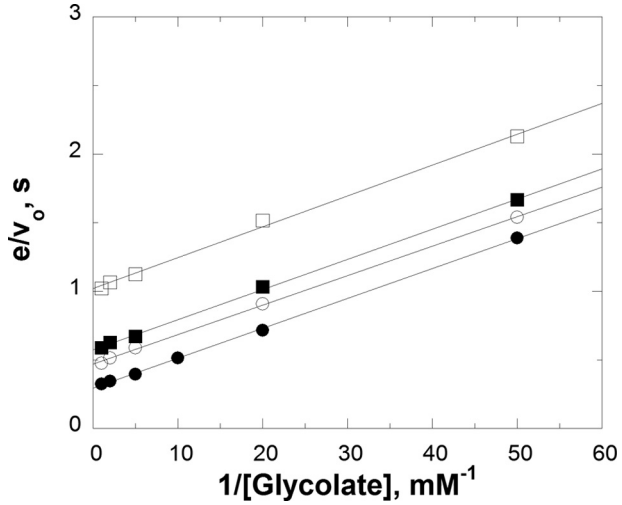

FIGURE 4. **Glyoxylate inhibition of human liver GOX with glycolate as substrate.** Double reciprocal plot of the steady-state kinetic data determined in 100 mM sodium phosphate, pH 7.0, at 30 °C and atmospheric oxygen concentration. Concentrations of glyoxylate were as follows: 0 mM (●), 0.5 mM (○), 1 mM (■), and 2.5 mM (□). Data derived by steady-state kinetic were fit to Equation 2.

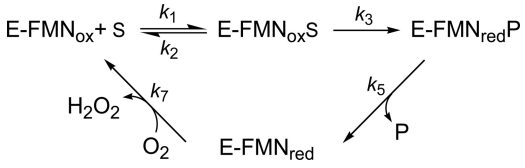

SCHEME 2. **Minimal steady-state kinetic mechanism of human liver GOX.** *E-FMN$_{ox}$*, oxidized enzyme; *E-FMN$_{red}$*, reduced enzyme; *S*, glycolate; *P*, glyoxylate.

kinetic pattern establishes that glycolate and glyoxylate bind to two forms of enzymes that are interconnected by the presence of at least one irreversible step (27). This immediately rules out product release occurring after reaction of the reduced enzyme with oxygen, since if this were the case, glyoxylate would compete with glycolate for binding to the same oxidized enzyme species. As illustrated in the minimal kinetic mechanism of Scheme 2, the inhibition data are consistent with release of glyoxylate from the reduced enzyme occurring prior to the oxidation of the reduced enzyme by molecular oxygen and with the chemical step of glycolate oxidation being irreversible (27). The relevant kinetic parameters determined were as follows: $k_{\mathrm{cat(app)}} = 3.32 \pm 0.03\ \mathrm{s}^{-1}$, $K_{\mathrm{glycolate(app)}} = 0.07 \pm 0.01$ mM, and $K_{ii(\mathrm{app})} = 1.05 \pm 0.02$ mM ($R^2 = 0.998$).

Upon mixing anaerobically GOX with glycolate in a stopped-flow spectrophotometer at pH 7.0 and 30 °C, reduction of the enzyme-bound flavin to the anionic hydroquinone state was observed as bleaching of the absorbance signal at 450 nm in a biphasic pattern (Fig. 5). Accordingly, the rapid kinetic data were fit best with a double exponential process (Equation 5). The observed rates for the first observable kinetic phase (k_{obs1}), which accounted for ~90% of the total absorbance change, were hyperbolically dependent on glycolate concentration. Fitting of the kinetic data to Equation 6, which describes a mechanism with a reversible chemical step of flavin reduction, yielded a limiting rate constant for flavin reduction (k_3) of 54 ± 1 s^{-1}, a $K_{d(\mathrm{app})}$ value of 0.29 ± 0.02 mM, and a limiting rate constant for the reverse of the chemical step of flavin reduction

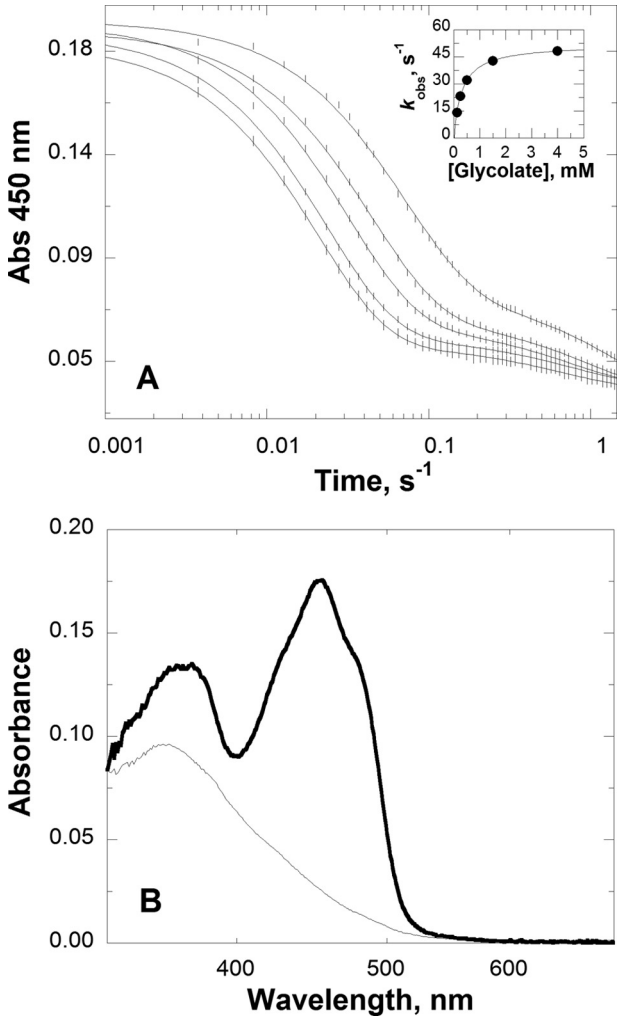

FIGURE 5. **Anaerobic reduction of human liver GOX with glycolate as substrate.** Reactions were carried out in a stopped-flow spectrophotometer in 100 mM sodium phosphate, pH 7.0, at 30 °C. *A*, time courses of the reaction at 450 nm obtained by anaerobic mixing of ~15 μM GOX and (from *left* to *right*) 4.0, 1.5, 0.5, 0.25, and 0.13 mM glycolate, respectively. All traces were fitted to Equation 5. The time indicated is after the end of flow (*i.e.* ~2 ms). For clarity, one experimental point out of every 10 is shown (*vertical lines*). The *inset* shows the hyperbolic dependence of the observed rates for the fast phase of flavin reduction (k_{obs1}) on the concentration of glycolate. Data were fit to Equation 7. *B*, the *thick curve* represents the UV-visible absorbance spectrum recorded ~2 ms after mixing anaerobically GOX with glycolate (*i.e.* oxidized enzyme before flavin reduction); the *thin curve* is the UV-visible absorbance spectrum recorded at the end of the reaction between GOX with glycolate (*i.e.* reduced enzyme).

(k_{rev}) that was not significantly different from zero (*i.e.* −1.8 ± 1.4 s^{-1}). In agreement with a negligible k_{rev} value, similar k_3 and $K_{d(\mathrm{app})}$ values were determined upon fitting the kinetic data to Equation 7, where the chemical step of flavin reduction is set to be irreversible (*i.e.* k_3 was 52 ± 0.4 s^{-1}, and $K_{d(\mathrm{app})}$ was 0.32 ± 0.01 mM). The observed rates for the second observable kinetic phase of flavin reduction (k_{obs2}), which accounted for only ~10% of the total change in absorbance at 450 nm, were independent of the concentration of glycolate with values between 1.1 and 1.3 s^{-1}. The observation that the k_{cat} value was at least 10 times larger than the k_{obs2} values suggests that the second phase of flavin reduction observed in the stopped-flow is not on the main catalytic pathway of the enzyme and is probably due to

minor heterogeneity in the enzyme preparation or a slow conformational change that occurs in the absence of oxygen.

The effect of solvent viscosity on the $k_{cat}/K_{glycolate}$ values for GOX was investigated to probe whether binding of the substrate to the enzyme occurs in rapid equilibrium and to establish whether the measured $K_{d(app)}$ incorporates not only the kinetic steps of substrate binding (k_1 and k_2) but also the kinetic step of flavin reduction (k_3) (28, 29). Initial rates of reaction were measured at varying concentrations of glycolate and atmospheric oxygen at pH 7.0 and 30 °C in the presence of various amounts of glycerol as viscosigen. As shown in Fig. 6, a slope of 0.23 ± 0.04 was determined in a plot of normalized $k_{cat}/K_{glycolate}$ values as a function of the relative viscosity of the solvent, suggesting that the binding of glycolate to GOX is not in rapid equilibrium (*i.e.* k_2 is comparable with k_3). These data also indicate that $K_{d(app)}$ measured in the reductive half-reaction is equal $(k_2 + k_3)/k_1$.

pH Dependences of Kinetic Parameters—The steady-state and pre-steady-state kinetic parameters were determined in the pH range from pH 5.0 to 10.0, in order to gain insight into whether ionizable groups participate in the kinetic steps of the mechanism of GOX. As in the case of pH 7.0, at any given pH value, the steady-state kinetic mechanism was Ping-Pong Bi-Bi (data not shown), and the stopped-flow traces describing the anaerobic substrate reduction of the flavin were biphasic, with the first phase accounting for more than 85% of the total change in absorbance (see supplemental Fig. S1). The kinetic parameters determined at different pH values using the steady-state kinetic approach are summarized in Table 1. Those for the anaerobic reductive half-reactions are listed in Table 2. Below pH 7.0, the enzyme was not saturated with oxygen at concentrations as high as 1 mM, thereby preventing the determination of the k_{cat} and K_{oxygen} values. Both the k_{cat} and k_3 values were independent of pH above pH 7.0 but showed slight decreases at pH 6.0 (k_{cat}) and pH 5.0 (k_3) (Fig. 7), consistent with the requirement of an unprotonated group acting as a base in the chemical step of glycolate oxidation.

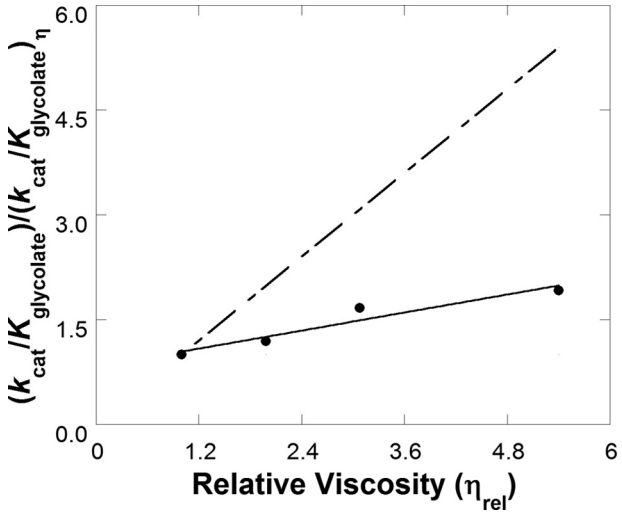

FIGURE 6. **Effect of solvent viscosity on the $k_{cat}/K_{glycolate}$ values for human liver GOX.** The *dashed line* with a slope of 1 describes a case in which the reaction is diffusion-controlled. GOX activity was measured at varying concentration of glycolate and atmospheric oxygen at 30 °C in 100 mM sodium phosphate, pH 7.0, in the absence and presence of glycerol as viscosigen. The *solid line* represents a fit of the data to Equation 9.

As shown in Fig. 7, the $k_{cat}/K_{glycolate}$ was maximal at low pH, with a limiting value of 74,000 ± 8,500 M^{-1} s^{-1}, and decreased with increasing pH values, defining an apparent pK_a value of 8.5 ± 0.1 for a group that needs to be protonated. In contrast, the $K_{d(app)}$ value for binding of glycolate to the enzyme was maximal at low pH, with a limiting value of 0.35 ± 0.04 mM, and increased with increasing pH values, defining an apparent pK_a value of 8.5 ± 0.1 for a group that needs to be protonated for substrate binding (Fig. 7). Finally, the pH profile for the k_{cat}/K_{oxygen} value increased from a poorly defined limiting value of 6,700 ± 2,000 M^{-1} s^{-1} at low pH to a well defined limiting value of 57,400 ± 4,700 M^{-1} s^{-1} at high pH, identifying a pK_a value of 6.8 ± 0.2 for a group that needs to be unprotonated for efficient oxidation of the reduced flavin by oxygen (Fig. 7). Interestingly, at any given pH value between 5.0 and 10.0, the UV-visible absorbance spectrum of the enzyme seen at the end of the substrate reduction process showed a well defined peak at ~340 nm (Fig. 6 and supplemental Fig. S1), consistent with the enzyme-bound reduced flavin being present in the anionic form throughout the pH range considered.

Attempt at Investigating the Mechanistic Role of His^{260}—The H260Q and H260A enzymes were expressed and purified to high levels following the protocol employed for the wild-type enzyme. Although ~2 mg of purified enzymes were obtained out of 1 g of wet cell paste, both enzyme variants did not show any absorbance in the 350–500 nm region, suggesting a lack of enzyme-bound flavin. In agreement with this observation, the apoenzymes did not show any oxygen consumption when assayed at final concentrations as high as 20 μM with 10 mM glycolate at pH 7.0 and 30 °C, irrespective of whether exogenous FMN as high as 400 μM was present in the enzyme reaction mixture. Independent attempts to measure oxygen consumption during catalytic turnover of the variant enzymes with

TABLE 1

Steady-state kinetic parameters for recombinant GOX with glycolate as a substrate between pH 6.0 and 10.0

Steady-state parameters were measured at varying concentrations of both organic substrate and oxygen at 30 °C. Rates are expressed per active site oxidized flavin content.

pH	k_{cat}	$K_{glycolate}$	K_{oxygen}	$k_{cat}/K_{glycolate}$	k_{cat}/K_{oxygen}
	s^{-1}	mM	mM	M^{-1} s^{-1}	M^{-1} s^{-1}
6.0		0.28 ± 0.01		54,300 ± 200	9,700 ± 100
6.5		0.25 ± 0.03		78,500 ± 12,100	13,000 ± 2,100
7.0	15.7 ± 0.4	0.23 ± 0.01	0.64 ± 0.03	68,300 ± 3,500	24,500 ± 1,300
7.5	20.0 ± 0.4	0.20 ± 0.01	0.44 ± 0.02	99,800 ± 5,400	45,400 ± 2,300
8.0	24.3 ± 1.0	0.50 ± 0.03	0.60 ± 0.05	48,600 ± 3,500	40,500 ± 3,800
8.5	24.1 ± 1.2	0.54 ± 0.05	0.40 ± 0.04	44,700 ± 4,700	60,300 ± 6,700
9.0	31.2 ± 0.1	2.00 ± 0.01	0.59 ± 0.01	15,600 ± 100	52,900 ± 100
9.5	28.5 ± 0.1	3.10 ± 0.01	0.39 ± 0.01	9,200 ± 100	73,200 ± 200
10.0	29 ± 2	13.7 ± 1.3	0.61 ± 0.07	2,100 ± 300	48,000 ± 6,400

TABLE 2

Reductive half-reaction of recombinant GOX with glycolate as a substrate between pH 5.0 and 10.0

Flavin reduction was carried out in a stopped-flow spectrophotometer at 30 °C. Pre-steady-state kinetic parameters were determined by fitting the data acquired upon mixing anaerobically the enzyme with glycolate to Equation 7.

pH	k_3	$K_{d(app)}$
	s^{-1}	mM
5.0	26.8 ± 0.2	0.66 ± 0.02
6.0	45.9 ± 0.3	0.41 ± 0.01
7.0	52.0 ± 0.4	0.32 ± 0.01
8.0	43.8 ± 0.2	0.39 ± 0.01
9.0	39.9 ± 0.2	1.64 ± 0.03
10.0	34.6 ± 0.5	9.35 ± 0.38

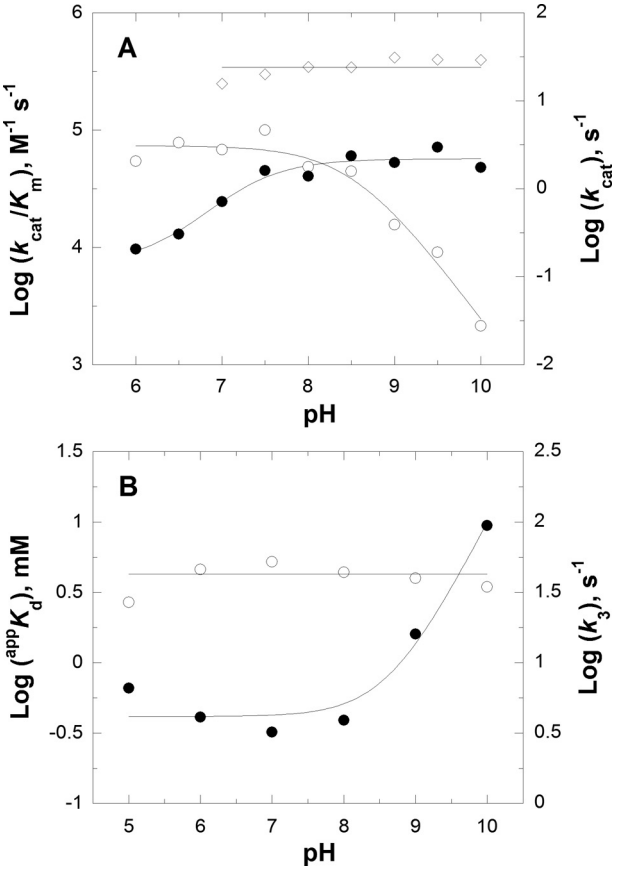

FIGURE 7. **pH profiles for the steady-state and pre steady-state kinetic parameters of human liver GOX with glycolate as substrate.** *A*, pH dependences of the k_{cat} (◇), $k_{cat}/K_{glycolate}$ (○), and k_{cat}/K_{oxygen} (●) values determined by using the steady-state approach with glycolate as substrate for GOX. Enzymatic activity assays were measured at varying concentration of both glycolate and oxygen between pH 6.0 and 10.0, at 30 °C. The curves were obtained by fitting the kinetic data to Equation 3 for the $k_{cat}/K_{glycolate}$ values and Equation 4 for the k_{cat}/K_{oxygen} values. *B*, pH dependence of the k_3 (○) and $K_{d(app)}$ (●) values determined by using stopped-flow spectrophotometry. The *curve* represents the fit of the kinetic data to Equation 8.

glycolate as substrate upon preincubating the H260Q or H260A apoenzymes with 1 mM FMN were also unsuccessful. Thus, the mechanistic investigation of the role of His^{260} in the reaction catalyzed by human liver GOX could not be carried out.

DISCUSSION

The renewed interest in human GOX arises from the potential for using the enzyme as drug target for the treatment of primary hyperoxaluria, a hereditary disorder in which large deposits of calcium oxalate produced enzymatically by GOX result in kidney stones (12). Despite a number of biochemical and structural studies on GOX from human and plants (9, 13–19, 23, 30–32), investigations aimed at the understanding of the mechanistic properties of the human enzyme have not been reported to date. Here, we have determined the effects of pH on the steady-state and pre-steady-state kinetic parameters of human liver GOX. The information that has emerged from these studies allowed us to establish that the enzyme shows a Ping-Pong Bi-Bi catalytic mechanism throughout the pH range from 6.0 to 10.0. The requirements for ionizable groups or lack thereof in all of the kinetic steps that define the minimal steady-state kinetic mechanism of the enzyme in turnover with glycolate have also been established.

The oxidation of glycolate to glyoxylate catalyzed by human liver GOX involves the flavin-mediated transfer of a hydride equivalent from the α-hydroxy acid substrate to the final electron acceptor oxygen. A Ping-Pong Bi-Bi mechanism is consistent with the kinetic data observed with glycolate as substrate for the enzyme, as illustrated in the minimal steady-state kinetic mechanism of Scheme 2. After the reversible formation of a Michaelis complex involving the oxidized enzyme and the substrate (E-FMN_{ox}·S), the enzyme reacts with glycolate irreversibly to generate glyoxylate with concomitant reduction of the enzyme-bound flavin (E-FMN_{red}·P). The catalytic cycle is then completed with the release of the glyoxylate product of the reaction from the active site of the enzyme (k_5 step in Scheme 2), followed by the second-order reaction of the reduced enzyme-bound FMN with molecular oxygen to generate hydrogen peroxide and oxidized enzyme (k_7 step). Evidence supporting the mechanism of Scheme 2 comes from the patterns with parallel lines that were observed in double reciprocal plots of the initial rates of reaction and the concentrations of either glycolate or oxygen. The Ping-Pong Bi-Bi kinetic mechanism was further confirmed with inhibition studies with glyoxylate. Indeed, the uncompetitive inhibition pattern observed is consistent with glycolate and glyoxylate binding to two forms of GOX, the oxidized and reduced enzymes, respectively, interconnected by an irreversible kinetic step of catalysis (*i.e.* the oxidation step where glycolate is converted to glyoxylate) (27). Further evidence for the chemical step of glycolate oxidation (k_3) being irreversible comes from the rapid kinetics data showing a negligible y intercept of the saturation curve that fits the reductive half-reaction data in a plot of k_{obs} *versus* [glycolate]. Although a Ping-Pong Bi-Bi steady-state kinetic mechanism was recently reported for human liver GOX at pH 7.0 and 7.5 (11, 23) and for the spinach enzyme at pH 8.3 (17), the investigation reported here shows that the relative order of the kinetic steps in the kinetic mechanism of the enzyme remains the same throughout the pH range from 6.0 to 10.0. In this respect, GOX has a behavior that is different from that previously reported for pyranose 2-oxidase, another flavin-dependent enzyme that oxidizes alcohols. In that case, the enzyme switches from a Ping-Pong Bi-Bi mechanism where flavin oxidation occurs after the release of the product at pH <7.0 to a ternary complex mechanism where oxidation of the flavin occurs while the product of the reaction is still bound at the active site at pH >7.0 (33).

A protonated group with an apparent pK_a value of 8.5 is required for the formation of the enzyme-substrate complex. Evidence supporting this conclusion comes from the pH profiles determined with glycolate as substrate for the enzyme using the steady-state and rapid kinetic approaches. Indeed, the $K_{d(app)}$ value, which due to substrate binding to the enzyme not being in rapid equilibrium equals $(k_2 + k_3)/k_1$, increased with increasing pH values. Since the kinetic step of glycolate oxidation defined by the rate constant k_3 is independent of pH above pH 7.0, any pH effect observed in this pH range on the $K_{d(app)}$ values necessarily arises from binding of the substrate to the active site of the enzyme. Interestingly, the requirement for the same protonated group with an apparent pK_a value of 8.5 is also seen in the pH profile for the steady-state second-order rate constant for capture of glycolate, $k_{cat}/K_{glycolate}$. In this case, lack of any pK_a value above pH 7.0 in the pH profile for the k_{cat} value establishes the apparent pK_a of 8.5 seen in the pH profile of the $k_{cat}/K_{glycolate}$ value as being due to a group participating in the formation of the enzyme-substrate complex but not catalysis (34). In the crystal structure of human liver GOX in complex with glyoxylate (20), the interaction between the enzyme and glyoxylate is mediated by several hydrogen bond and electrostatic interactions involving ionizable groups of the protein, including Tyr^{26}, Arg^{167}, and Arg^{263} (Fig. 1) (20). Although mechanistic data on site-directed mutants are not available on the human liver enzyme, substitution of Tyr^{24} with phenylalanine in spinach GOX, which is equivalent to Tyr^{26} of the human enzyme, resulted in a 20-fold increase in the K_d value for glycolate, suggesting that the active site tyrosine perhaps participates in substrate binding (19).

An ionizable group with an undefined pK_a value that must be lower than 5.0 needs to be unprotonated in the catalytic step of flavin reduction, as suggested by the pH effects on the rate constant for anaerobic flavin reduction (k_3) when human liver GOX is mixed with glycolate in a stopped-flow spectrophotometer. Independent support for this conclusion comes from the pH independence of the overall turnover of the enzyme under steady-state conditions. These results are in keeping with the hydride ion transfer mechanism that was recently proposed for another member of the α-hydroxy acid oxidase superfamily, flavocytochrome b_2, based on primary and solvent deuterium kinetic isotope effects on the wild type and selected active site mutant enzymes (35–37). The results are also consistent with the alternative proposal that the initial abstraction of a proton is not occurring on the hydroxyl group of glycolate but instead on the substrate α-carbon to generate an activated carbanion species that goes on to form a covalent intermediate with the N(5) atom of the enzyme-bound FMN, as previously proposed by other groups for flavocytochrome b_2 and mandelate dehydrogenase (5, 19, 38, 39). Irrespective of the mechanism of substrate activation (*i.e.* through formation of a substrate alkoxide or a carbanion intermediate), a histidine residue that is highly conserved throughout the α-hydroxy acid oxidase superfamily is found in the active site of human liver GOX that could serve as the proton acceptor for the activation of glycolate, namely His^{260} (Fig. 1) (20). In this regard, replacement of the homologous histidine with glutamine in lactate monooxygenase decreased the rate constant for anaerobic flavin reduction by 7 orders of magnitude, consistent with the conserved histidine acting as an active site base (40). Recent mechanistic data on the equivalent histidine residue found in the active site of flavocytochrome b_2 (37, 41) suggest that in that enzyme, the active site histidine plays a dual role in maintaining the integrity of the active site for catalysis and as a proton acceptor in the reaction catalyzed by the enzyme. As shown in this study, the replacement of the conserved histidine in human liver GOX has a major effect on FMN retention, preventing a mechanistic investigation of the role of His^{260} in catalysis.

Some kinetic step other then the chemical step of catalysis is partially contributing to the overall rate of turnover of the enzyme at pH values lower than 7.0 but not at high pH values. At high pH, the similarity between the k_3 and k_{cat} values (*i.e.* 35 and 29 s^{-1}, respectively, at pH 10.0) establishes the oxidation of the glycolate to glyoxylate as being the major rate-limiting kinetic step for the overall turnover of the enzyme. This is clearly not the case at pH 7.0, where the k_{cat} value is significantly lower than the k_3 value (*i.e.* 17 s^{-1} as compared with 52 s^{-1}). For the minimal steady-state kinetic mechanism of Scheme 2, the overall turnover of the enzyme at saturating concentrations of the substrates includes all of the kinetic steps other than the second-order steps, where glycolate binds to the enzyme and oxygen reacts with the reduced enzyme (42). Therefore, it is likely that at low pH, the release of glyoxylate from the active site of the enzyme is at least partially rate-determining for the overall turnover of the enzyme. However, it cannot be ruled out *a priori* that a first-order kinetic step included in the oxidative half-reaction in which the reduced flavin reacts with oxygen (*i.e.* k_7 in Scheme 2) and that is undetectable when using the steady-state approach may contribute to the overall turnover of the enzyme at pH values lower than 7.0.

The reaction of the reduced flavin of human liver GOX with molecular oxygen is an order of magnitude faster when a group with apparent pK_a of 6.8 is unprotonated. This conclusion is supported by the pH profile of the second-order rate constant k_{cat}/K_{oxygen} determined under steady-state kinetics conditions, which increased from a limiting value of ~7,000 M^{-1} s^{-1} at low pH to a limiting value of ~60,000 M^{-1} s^{-1} at high pH values. The limiting value in the upper 10^4 M^{-1} s^{-1} range seen at high pH is in keeping with values previously reported for other flavoprotein oxidases, such as, for example, spinach GOX (17), choline oxidase (43, 44), monoamine oxidase (45, 46), nitroalkane oxidase (47), lactate oxidase (48), sarcosine oxidase (49), and glucose oxidase (50), and it is ~2.5 orders of magnitude larger than the value of 2.5×10^2 M^{-1} s^{-1} that was reported for the non-enzymatic oxidation of flavins in solutions (48, 51). However, the pH profile for the k_{cat}/K_{oxygen} value for GOX is significantly different from the pH profiles of the k_{cat}/K_{oxygen} values that were previously reported for glucose oxidase and choline oxidase. In glucose oxidase, effective oxidation of the reduced flavin was proposed to require an active site histidine with pK_a of 7.9 to be protonated (50, 52). In choline oxidase, oxidation of the reduced flavin is facilitated by the non-dissociable, positively charged trimethylammonium moiety of the choline substrate but not by ionizable groups in the active site of the enzyme (43, 53–55). In GOX, one can immediately rule out the ionization of the flavin hydroquinone species as being

responsible for the pK_a value of 6.8, since the UV-visible absorbance spectra of the reduced enzyme after anaerobic reaction with glyoxylate, with well resolved maxima at ~340 nm, strongly support the notion that the hydroquinone species is in the anionic state between pH 6.0 and 10.0 (56). At this stage of the investigation, we can only speculate that the pK_a of 6.8 may reflect a kinetic pK_a value defining a change in the rate-limiting step that governs reactivity of the reduced flavin with oxygen. Alternatively, the pK_a of 6.8 may reflect a thermodynamic equilibrium for the interconversion of two enzyme forms that react differently with oxygen. Future studies will be required to further elucidate the interesting reactivity of human GOX with molecular oxygen.

In conclusion, in this study, the pH profiles of the steady-state and pre-steady-state kinetic parameters of human liver GOX have been examined. The enzyme showed a Ping-Pong Bi-Bi mechanism throughout the pH range from 6.0 to 10.0. Formation of the enzyme-substrate complex is favored at pH values lower than 8.5, whereas the chemical step in which the flavin is reduced by glycolate is faster at pH values above 7.0. Finally, the reaction of the reduced flavin with molecular oxygen showed a pH profile that is unprecedented in flavoprotein oxidases and that complements the cases previously reported for glucose oxidase and choline oxidase. The results of the mechanistic investigation presented here thereby define a platform for future mechanistic studies of human liver GOX and raise important questions that will require attention, such as, for example, what the mechanism is for the activation of the organic substrate and of molecular oxygen for reaction with the enzyme-bound flavin catalyzed by GOX.

Acknowledgments—We thank Prof. Alessio Peracchi (University of Parma, Italy) for the generous gift of plasmid pTrcHisB-HAOX1 harboring the gene encoding for human glycolate oxidase. We thank William S. Jonas, M.D., and all of the other doctors and nurses at Piedmont Hospital (Atlanta, GA) for help.

REFERENCES

1. Fry, D. W., and Richardson, K. E. (1979) *Biochim. Biophys. Acta* **568,** 135–144
2. Blanchard, D. E., Nocito-Carrol, V., and Ratner, S. (1946) *J. Biol. Chem.* **163,** 137–144
3. Belmouden, A., Lê, K. H., Lederer, F., and Garchon, H. J. (1993) *Eur. J. Biochem.* **214,** 17–25
4. Maeda-Yorita, K., Aki, K., Sagai, H., Misaki, H., and Massey, V. (1995) *Biochimie* **77,** 631–642
5. Lehoux, I. E., and Mitra, B. (1999) *Biochemistry* **38,** 9948–9955
6. Jacq, C., and Lederer, F. (1972) *Eur. J. Biochem.* **25,** 41–48
7. Nishimura, M., Akhmedov, Y. D., Strzalka, K., and Akazawa, T. (1983) *Arch. Biochem. Biophys.* **222,** 397–402
8. Tolbert, N. E., Clagett, C. O., and Burris, R. H. (1949) *J. Biol. Chem.* **181,** 905–914
9. Schuman, M., and Massey, V. (1971) *Biochim. Biophys. Acta* **227,** 500–520
10. Kun, E., Dechary, J. M., and Pitot, H. C. (1954) *J. Biol. Chem.* **210,** 269–280
11. Schwam, H., Michelson, S., Randall, W. C., Sondey, J. M., and Hirschmann, R. (1979) *Biochemistry* **18,** 2828–2833
12. Holmes, R. P. (1998) *J. Nephrol.* **11,** Suppl. 1, 32–35
13. Lindqvist, Y. (1989) *J. Mol. Biol.* **209,** 151–166
14. Lindqvist, Y., and Brändén, C. I. (1979) *J. Biol. Chem.* **254,** 7403–7404
15. Lindqvist, Y., and Brändén, C. I. (1985) *Proc. Natl. Acad. Sci. U.S.A.* **82,** 6855–6859
16. Macheroux, P., Kieweg, V., Massey, V., Söderlind, E., Stenberg, K., and Lindqvist, Y. (1993) *Eur. J. Biochem.* **213,** 1047–1054
17. Macheroux, P., Massey, V., Thiele, D. J., and Volokita, M. (1991) *Biochemistry* **30,** 4612–4619
18. Macheroux, P., Mulrooney, S. B., Williams, C. H., Jr., and Massey, V. (1992) *Biochim. Biophys. Acta* **1132,** 11–16
19. Stenberg, K., Clausen, T., Lindqvist, Y., and Macheroux, P. (1995) *Eur. J. Biochem.* **228,** 408–416
20. Murray, M. S., Holmes, R. P., and Lowther, W. T. (2008) *Biochemistry* **47,** 2439–2449
21. Mowat, C. G., Beaudoin, I., Durley, R. C., Barton, J. D., Pike, A. D., Chen, Z. W., Reid, G. A., Chapman, S. K., Mathews, F. S., and Lederer, F. (2000) *Biochemistry* **39,** 3266–3275
22. Xu, Y., Dewanti, A. R., and Mitra, B. (2002) *Biochemistry* **41,** 12313–12319
23. Vignaud, C., Pietrancosta, N., Williams, E. L., Rumsby, G., and Lederer, F. (2007) *Arch. Biochem. Biophys.* **465,** 410–416
24. Williams, E., Cregeen, D., and Rumsby, G. (2000) *Biochim. Biophys. Acta* **1493,** 246–248
25. Allison, R. D., and Purich, D. L. (1979) *Methods Enzymol.* **63,** 3–22
26. Lide, D. R. (ed) (2000) *CRC Handbook of Chemistry and Physics*, pp. 8–57, CRC Press, Inc., Boca Raton, FL
27. Cleland, W. W. (1963) *Biochim. Biophys. Acta* **67,** 188–196
28. Lutz, S., and Bornscheuer, T. U. (eds) (2009) *Protein Engineering Handbook*, Vol. 1, pp. 8–10, Wiley-VCH, Weinheim, Germany
29. Strickland, S., Palmer, G., and Massey, V. (1975) *J. Biol. Chem.* **250,** 4048–4052
30. Ushijima, Y. (1973) *Arch. Biochem. Biophys.* **155,** 361–367
31. Duley, J., and Holmes, R. S. (1974) *Genetics* **76,** 93–97
32. Stenberg, K., and Lindqvist, Y. (1997) *Protein Sci.* **6,** 1009–1015
33. Rungsrisuriyachai, K., and Gadda, G. (2009) *Arch. Biochem. Biophys.* **483,** 10–15
34. Cleland, W. W. (1982) *Methods Enzymol.* **87,** 390–405
35. Sobrado, P., Daubner, S. C., and Fitzpatrick, P. F. (2001) *Biochemistry* **40,** 994–1001
36. Sobrado, P., and Fitzpatrick, P. F. (2003) *Biochemistry* **42,** 15208–15214
37. Tsai, C. L., Gokulan, K., Sobrado, P., Sacchettini, J. C., and Fitzpatrick, P. F. (2007) *Biochemistry* **46,** 7844–7851
38. Pompon, D., and Lederer, F. (1985) *Eur. J. Biochem.* **148,** 145–154
39. Urban, P., and Lederer, F. (1984) *Eur. J. Biochem.* **144,** 345–351
40. Müh, U., Williams, C. H., Jr., and Massey, V. (1994) *J. Biol. Chem.* **269,** 7989–7993
41. Gaume, B., Sharp, R. E., Manson, F. D., Chapman, S. K., Reid, G. A., and Lederer, F. (1995) *Biochimie* **77,** 621–630
42. Cleland, W. W. (1975) *Biochemistry* **14,** 3220–3224
43. Ghanem, M., Fan, F., Francis, K., and Gadda, G. (2003) *Biochemistry* **42,** 15179–15188
44. Fan, F., and Gadda, G. (2005) *J. Am. Chem. Soc.* **127,** 2067–2074
45. Tan, A. K., and Ramsay, R. R. (1993) *Biochemistry* **32,** 2137–2143
46. Miller, J. R., and Edmondson, D. E. (1999) *J. Biol. Chem.* **274,** 23515–23525
47. Gadda, G., and Fitzpatrick, P. F. (2000) *Biochemistry* **39,** 1406–1410
48. Massey, V. (1994) *J. Biol. Chem.* **269,** 22459–22462
49. Wagner, M. A., and Jorns, M. S. (2000) *Biochemistry* **39,** 8825–8829
50. Roth, J. P., and Klinman, J. P. (2003) *Proc. Natl. Acad. Sci. U.S.A.* **100,** 62–67
51. Mattevi, A. (2006) *Trends Biochem. Sci.* **31,** 276–283
52. Su, Q., and Klinman, J. P. (1999) *Biochemistry* **38,** 8572–8581
53. Gadda, G., Fan, F., and Hoang, J. V. (2006) *Arch. Biochem. Biophys.* **451,** 182–187
54. Ghanem, M., and Gadda, G. (2005) *Biochemistry* **44,** 893–904
55. Rungsrisuriyachai, K., and Gadda, G. (2008) *Biochemistry* **47,** 6762–6769
56. Ghisla, S., Massey, V., Lhoste, J. M., and Mayhew, S. G. (1974) *Biochemistry* **13,** 589–597